Songklanakarin J. Sci. Technol.
42 (2), 439-446, Mar. - Apr. 2020

http://www.sjst.psu.ac.th

Original Article

TiO_2/ZnO nanocomposite photocatalyst: Synthesis, characterization and their application for degradation of humic acid from aqueous solution

Muhammad Ali Zulfikar[1*], Anggia D. Chandra[1], Rusnadi[1], Henry Setiyanto[1], Nurrahmi Handayani[1], and Deana Wahyuningrum[2]

[1] *Analytical Chemistry Research Group, Bandung Institute of Technology, Bandung, Jawa Barat, 40132 Indonesia*

[2] *Organic Chemistry Research Group, Bandung Institute of Technology, Bandung, Jawa Barat, 40132 Indonesia*

Received: 1 October 2018; Revised: 18 January 2019; Accepted: 27 January 2019

Abstract

In this study, TiO_2/ZnO nanocomposite (TZC) photocatalysts were successfully prepared through a sol-gel process followed by calcination. TZC photocatalyst characterization was performed by XRD, FTIR, SEM, TEM and UV-vis diffuse reflectance spectroscopy (DRS). The photocatalytic activity of the TZC photocatalyst is studied systematically by the degradation of humic acid (HA) from aqueous solutions under visible light irradiation. Photodegradation of HA from aqueous solutions shows excellent photocatalytic activity. The rate of photocatalytic degradation increases with increasing catalyst loading and light intensity. From kinetic studies, it showed that HA photodegradation using TZC photocatalysts can be explained by the pseudo-first-order kinetic model. The results also show that this method has excellent potential to remove HA from peat water.

Keywords: humic acid, photocatalytic degradation, nanocomposite, TiO_2/ZnO, photocatalyst

1. Introduction

Humic materials are the major organic compounds contained in the peat water (Stevenson & Goh, 1971). Humic compounds can be described as negatively charged polyelectrolyte macromolecules because of the carboxylic and phenollic functional groups which are contained in their structure (Abbt-Braun, Frimmel, & Schulten, 1989). This property cause these compounds are difficult to degrade and potentially produce the other compounds with carcinogenic properties (Zouboulis, Chai, & Katsoyiannis, 2004). The compounds also have aromatic functional groups which contribute to the presence of color in the peat water (Moore, 1985). Conventional treatment processes include coagulation and flocculation (Lee, Morad, Teng, & Poh, 2012; Matilainen, Vepsäläinen, & Sillanpää, 2010; Ng *et al.*, 2012), membrane filtration (Lamsal, Montreuil, Kent, Walsh, & Gagnon, 2012; Metsämuuronen, Sillanpää, Bhatnagar, & Mänttäri, 2014), photocatalysis (Ng, Kho, Liu, Lim, & Amal, 2014; Philippe *et al.*, 2010) and adsorption techniques (Zulfikar *et al.*, 2016; Zulfikar, Afrianingsih, Nasir, & Handayani, 2017; Zulfikar, Afrita, Wahyuningrum, & Ledyastuti, 2016; Zulfikar, Wahyuningrum, Mukti, & Setiyanto, 2016) have been developed to remove these substances.

ZnO is being considered as an alternative material to TiO_2 because they have similar properties as a semiconductor. Moreover, ZnO exhibits a higher electron mobility and longer photo-generated electron lifetime than TiO_2, which is beneficial for photocatalytic degradation of dyes (Huang *et al.*, 2013). It can be synthesized by various synthesis methods (Huang *et al.*, 2013, Song, Zhang, Wu, & Wei, 2012; Uddin *et al.* 2012; Wang *et al.* 2011). However, it can only absorb a

*Corresponding author
Email address: zulfikar@chem.itb.ac.id

very small ultraviolet part of the solar spectrum because of its wide band gap, which is similar to TiO_2. Therefore, it is essential to develop new photocatalysts with a smaller band gap to harvest visible light.

In the present work an attempt was made to enhance the photocatalytic activity of ZnO by synthesizing of TiO_2 /ZnO using a sol-gel process followed by calcination treatment. Photocatalytic activity of TiO_2/ZnO nano composite (TZC) photocatalyst was evaluated by measuring the photodegradation of humic acid (HA) under visible light irradiation.

2. Materials and Methods

2.1 Materials

All materials were commercial reagent grade and used as received without further purification. The reagents used for the preparation of TZC photocatalyst were tetraethoxyortho titanate (TEOT) (Sigma-Aldrich), zinc acetate dehydrate (Sigma-Aldrich), citrate acid (Sigma-Aldrich), ethylene glycol (EG) (MW = 36,000) (Sigma-Aldrich). Deionized water was used in all experiments. For the photodegradation evaluated, humic acid (HA) (Sigma-Aldrich) was chosen as the model organic pollutant.

2.2 TiO_2/ZnO nano composite photocatalyst fabrication

A series of ZnO combined TiO_2 catalysts (abbreviated as TZC) with different concentrations of TiO_2 were prepared by changing the quantity of TEOT added to the ethanol. First, TEOT with various concentrations of Ti (1%, 3%, and 5%) in ethanol were mixed with 25 mmol of citric acid and stirred. Subsequently, a portion of $Zn(CH_3COO)_2 \cdot 2H_2O$ was added dropwise to the solution by sufficiently ultrasonic dispersing for 1 h at 80 °C to obtain a homogeneous solution. During the reaction, 5% (w/w) of polyethylene glycol (PEG) solution was added and stirred continuously until a light yellow sol was formed. The addition of PEG as additive was carried out to increase the nano composite performances (Khodadadi, Sabeti, Moradi, Azar, & Farshid, 2012). The catalysts were designated as TZC-X where "X" represents the nominal mass percentage content of TiO_2 in ZnO. Pure TiO_2 was prepared by the same procedure but by replacing the mixture solution with anhydrous ethanol. At last, the sol was dried at 80 °C for 6 h to reduce the solvents. The formed gel was then calcined in a furnace with temperature ramping slowly to 800 °C (at heating rate of 1 °C min^{-1}) and at 650 °C for 2 h to obtain a white solid nanocatalyst.

2.3 Material characterizations

The phase and crystallinity of TZC were studied by X-ray powder diffraction (XRD) with a Bruker D-8 Advance diffractometer with Cu kα radiation (40 kV, 30 mA). Identification of the phases was done with the help of the Joint Committee on Powder Diffraction Standards (JCPDS) files. The structure analysis of TZC photocatalyst was performed using a Shimadzu FTIR in the wave number range between 4000 and 450 cm^{-1}. The morphology of the TZC photocatalyst were investigated using scanning electron microscope with energy dispersive spectroscopy (SEM-EDS) (JEOL Model JSM 6360) and using high resolution transmission electron microscope (HRTEM, JEOL Model JEM 1400). The diffuse reflectance UV-Vis spectra (DRS) were recorded on a Thermo Scientific Evolution 220 system equipped with a Labsphere diffuse reflectance accessory to obtain the reflectance spectra of the catalysts over a range of 200-800 nm. $BaSO_4$ (Labsphere USRS-99-010) was used as a reference in the measurement. The measured spectra were converted from reflection to absorbance by the well-known Kubelka-Munk method.

2.4 Photocatalytic activity studies

The photocatalytic degradation of humic acid (HA) from aqueous solution in the presence of TZC photocatalyst was performed in a self-designed photo reactor at room temperature. Photocatalytic studies were performed to investigate the effect of TiO_2 composition in the photocatalyst, pH solution, distance of lamp from the material, power of lamp, and the comparison between photolysis, adsorption, and photocatalytic.

2.4.1 The effect of TiO_2 composition in the nanocomposite

Initially, a 100 mL of aqueous HA solution (25 mg/L) and 0.08 g TZC-1 were placed inside the reactor and was continuously stirred for 1 h and irradiated under Hg lamp (Philips) at 15 W. The HA solution was separated from the photocatalysts by centrifugation for 20 min to determine the concentration of HA using UV-Vis spectrophotometer model 1601 (Shimadzu, Japan) in the wavelength of 254 nm at various times of light exposure (0.5; 1; 1.5; 2; 2.5; and 3 h). The same procedure was carried out by changing TZC-1 with another material (TZC-3, TZC-5 and ZnO). The percentage of degradation efficiency was calculated by following Equation 1:

$$\%D = [(C_o - C_f)/C_o] \times 100\% \quad (1)$$

where *%D* was percentage of degradation, and *Co* and *Ct* were the HA concentration which were measured initially and at a certain time after irradiation, respectively.

2.4.2 Influence of the dosage of catalyst material

A 100 mL of HA solution (25 mg/L) was stirred continuously and irradiated by a Hg lamp (15 W) for 1 h. The measurement of HA concentration after irradiation was performed for each of dosages variation (in the range of 0.02-0.20 g) by UV-Vis spectrophotometer at 254 nm.

2.4.3 Effect of pH

A 100 mL of HA solution (25 mg/L) with various pH (pH 1-12) were added with TZC-1 (in accordance with the results obtained in testing of the nanocatalyst's amount effect). The photocatalytic process was carried out under Hg lamp (15 W) with continuously stirring for 1 h. HA concentration was measured by using UV-Vis spectrophotometer in the wavelength of 254 nm.

2.4.4 Effect of lamp distance from the surface of solution

A 100 mL of HA solution (25 mg/L) was mixed with TZC-1 (in optimum pH and dosage), continuously stirred for 1 h, and irradiated under Hg lamp (15 W). The test was carried out with varying the distance of lamp with the material surface (7.5; 11.5; and 15 cm). Concentration of HA was measured by using UV-Vis spectrophotometer in the wavelength of 254 nm.

2.4.5 Influence of Hg lamp power

A 100 mL of HA solution (25 mg/L) was mixed with TZC-1 (in optimum pH, dosage, and distance of lamp with the surface), continuously stirred for 1 h, and irradiated under Hg lamp (15 W). The test was carried out with varying the power of lamp (8; 10; and 15 W). Concentration of HA was measured by using UV-Vis spectrophotometer in the wavelength of 254 nm.

2.4.6 Comparison of photolysis, adsorption, and photocatalytic

A 100 mL of HA solution (25 mg/L) was continuously stirred and treated as follows: a) For photolysis, HA solution only stirred without nanocatalyst material addition and no irradiation; b) For adsorption, HA solution was added with TZC-1 0.08 g, without irradiation; c) For photocatalytic, HA solution was added with TZC-1 0.08 g and irradiated under Hg lamp (15 W). HA concentration measurements were performed on the three different conditions for 0.5; 1; 1.5; 2; 2.5; and 3 h by using UV-Vis spectrophotometer at 254 nm.

2.5 HA photodegradation from peat water (real sample)

Peat water samples containing HA as coexisting anions were collected from Rimbo Panjang, a sub district of Kampar in Riau Province, Indonesia, which is a source for water supply. Photodegradation of HA from peat water samples was performed using the batch systems and similar procedure described earlier. The peat water samples at original pH were fed onto the photo reactor and irradiated for various time of light exposure (0.5; 1; 1.5; 2; 2.5; and 3 h). Table 1 shows the characteristics of the peat water.

Table 1. Characteristics of the peat water

Parameters	Unit	Result
Color	Pt-Co	475
Organic compounds	mg/L $KMnO_4$	238
pH	-	4.01
Conductivity	µS/cm	62
Turbidity	mg/L SiO_2	7.5
Iron	mg/L	0
Manganese	mg/L	0
Calcium	mg/L	0
Magnesium	mg/L	6.2

3. Results and Discussion

3.1 Characterization of nano composite photocatalyst

3.1.1 XRD analysis

Investigation by X-ray diffraction was carried out to analyze the phase composition and crystallite size of the samples. The addition of Ti to ZnO affects the formation of the material.

Figure 1a shows the XRD pattern of both ZnO and TZC photocatalyst samples. The peak appears at 2θ =31.61°, 34.36°, 36.25°, 47.75°, 56.55°, 62.05°, 67.87°, 68.84°, and 72.54° correspond to the ZnO reference pattern (PDF: 96-230-114). In the TZC-3 and TZC-5 samples, after increasing the titanium oxide molar ratio, Ti and Zn were doped and the new

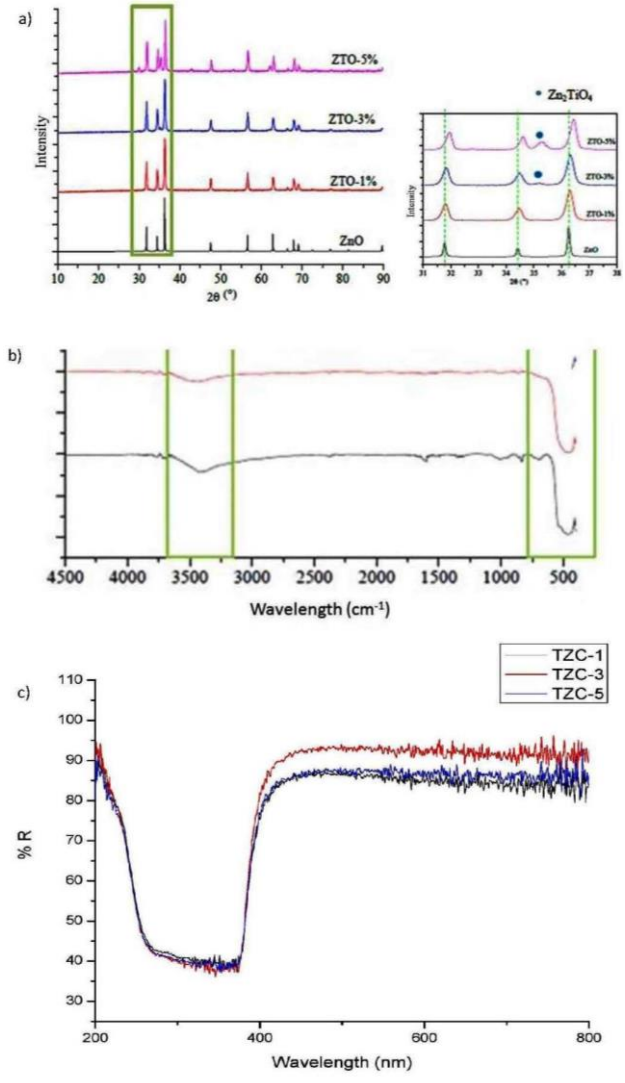

Figure 1. a) XRD patterns of ZnO and TZC photocatalyst; b) FTIR spectrum of ZnO (black) and TZC photocatalyst (red); c) DRS spectrum of TZC photocatalysts.

intense peaks were detected. The XRD line at 35.17° corresponds to Zn_2TiO_4, or to $ZnTi_{1.5}O_4$ (JCPDS 04-006-5709).

3.1.2 FTIR analysis

FTIR spectra of ZnO and TZC-1 are shown in Figure 1b. The broad band at 3400 cm^{-1} and the small band at 1600 cm^{-1} are related to the water and hydroxyl groups physically adsorbed in the sample (Ullah, Khan, & Khan, 2014; Pozan & Kambur, 2014; Khodadadi, Sabeti, Moradi, Azar, & Farshid, 2012). Absorption bands between 400 and 750 cm^{-1} are associated with symmetrical and asymmetrical stretching frequencies of the Zn-O and Ti-O vibrational bands (Ullah *et al.*, 2014; Stoyanova *et al.*, 2013).

3.1.3 UV-vis diffuse reflectance spectra analysis

The UV-vis diffuse reflectance spectra (DRS) of TZC-1, TZC-3 and TZC-5 were compared (Figure 1c). Using the well-known Kubelka-Munk equation, the band gap of pure ZnO and TZC-1, TZC-3 and TZC-5 were 3.22, 3.17, 3.18, and 3.18, respectively. There is a slight change in the band-gap energy among the TZC as prepared at different TiO_2 compositions. However, the decrease in TZC photocatalyst band gap energy can be attributed to the synergistic effect between the conduction bands of ZnO and TiO_2. Some sub-bands are formed by introducing impurities and defects to the forbidden band of TiO_2 thereby reducing the band-gap energy (Pei & Leung, 2013; Perkgoz *et al.*, 2011; Štengl, Bakardjieva, & Murafa, 2009).

3.1.4 SEM and TEM analysis

Morphology of the TZC photocatalyst was characterized by SEM as shown in Figure 2. The beam energy used in SEM experiments was 20 kV, which has been marked in the SEM image. The surface of as-spun, randomly oriented, TZC photocatalyst appears relatively smooth and uniform. In TZC-5, with a further increase in TiO_2, several large aggregations of different sizes were dispersed that decreased the photocatalytic activity.

TZC morphology in different TiO_2 compositions was also characterized by HRTEM. The surface morphology and size of the samples vary depending on the composition of Ti as shown in Figure 3. The TZC consists of compactly packed nanocrystallites surface and randomly oriented. Diameter of the nanocrystallites was calculated from HRTEM image (see Figure 3a-c). The diameter ranges from 84.22 to 185.95 nm for TZC-1, 62.53-134.81 nm for TZC-3 and 67.63-111.02 nm for TZC-5.

3.2 Photocatalytic studies

3.2.1 Effect of TiO_2 composition toward photocatalytic process

The photocatalytic activity of the pure ZnO and TZC was evaluated by the photocatalytic degradation of HA under visible light irradiation. From Figure 4a, it can be seen that the percentage of degradation decrease with increasing the TiO_2 content. The degradation percentage of ZnO, TZC-1, TZC-3, and TZC-5 were 80.63%, 89.43%, 88.58%, and 81.23%, respectively. In the TZC catalyst, photogeneration electron transfer occurs from the conduction band of light-activated ZnO to the conduction band of light-activated TiO_2 and, conversely, the transfer of holes can occur from the valence band of TiO_2 to the ZnO valence band (Pei & Leung, 2013; Sukharev & Kershaw, 1996). Meanwhile, due to the

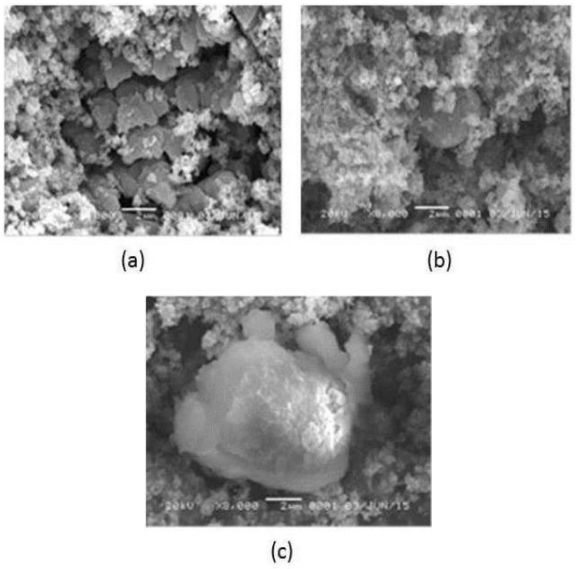

Figure 2. The SEM image of photocatalyst: (a) TZC-1, (b) TZC-3, (c) TZC-5

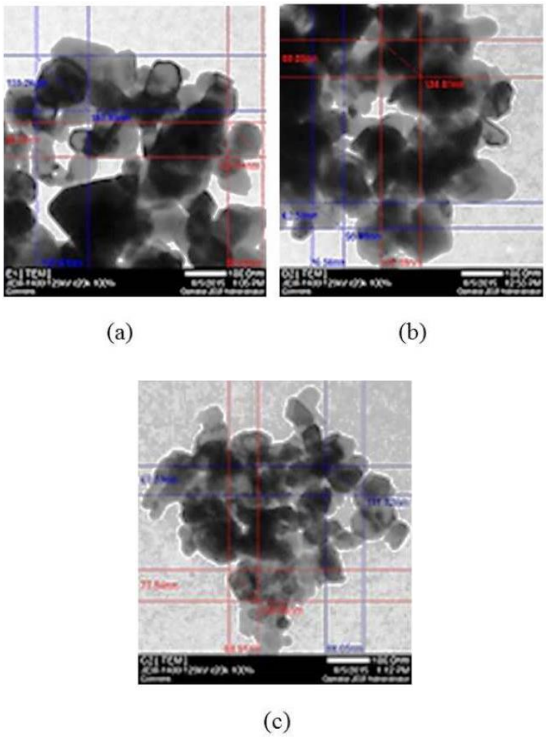

Figure 3. The HRTEM image of photocatalyst: (a) TZC-1, (b) TZC-3, (c) TZC-5

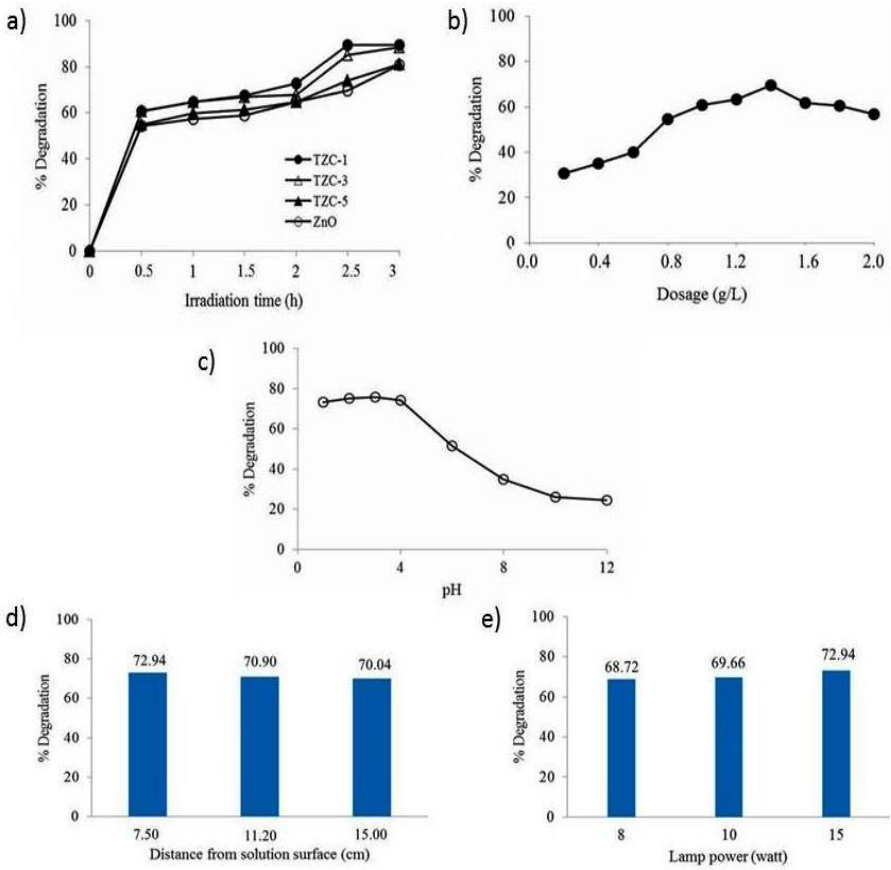

Figure 4. Effect of : a) TiO_2 composition toward percentage of HA degradation; b) dosage of catalyst material; e) pH; d) light distance from the surface of solution; and e) lamp power towards photocatalytic activity.

differences in the energy band position, there exists a synergetic relationship between ZnO, anatase and rutile to reduce the band-gap energy (Pei & Leung, 2013) and this could increase the photocatalytic activity of TZC. However, the addition of a high dose of the TiO_2 to ZnO causes the formation of photoinactive Zn_2TiO_4 compound (such as XRD analysis confirmed above) which will reduce photocatalytic activity (Janitabar-Darzi & Mahjoub, 2009; Moradi, Azar, Farshid, Khorrami, & Givianrad, 2012; Wang, Xu, Wang, & Zhao, 2005). From the results, it indicates that the nano-photocatalyst material with the most excellent photocatalytic ability is TZC-1.

3.2.2 Effect of catalyst dosage

The effect of catalyst dosage on photocatalytic activity is represented in Figure 4b. From the graph, the optimum dosage of catalyst which can be added during the photocatalytic process is 1.4 g/L. From 0.02 to 1.14 g/L, the percentage of HA degradation increase, but immediately decreased after adding more TZC-1. Under a low catalyst dosage, the degradation efficiency is enhanced by increasing the catalyst dosage due to the increasing number of active sites on the photocatalyst surface. Beyond a certain limit of catalyst dosage, the solution becomes turbid and thus blocks light radiation for the reaction to continue and therefore the percentage degradation starts to decrease (Pei & Leung, 2013). In addition, an increase in the amount of catalyst causes catalyst particle aggregation and this ends up in reducing the available surface area for light absorption. Similar results have been reported by (Evgenidou, Fytianos, & Poulios, 2005; Pei & Leung, 2013; Nagaveni, Sivalingam, Hegde, & Madras, 2004; Sobana & Swaminathan, 2007).

3.2.3 Effect of pH

The pH of an aquatic environment plays an important role in photocatalytic degradation of organic compounds because it determines the surface charge of the catalyst and the size of aggregate formed. Therefore, the pH of the solution can play a key role in photocatalytic oxidation of pollutants (Bansal, Chaudhary, & Mehta, 2015). The effect of pH value in the range from 4 to 10 on visible radiation degradation of HA was investigated under photoreaction with an initial HA concentration of 25 mg/L, 14 mg of TZC-1 and the results are shown in Figure 4c. The rate of degradation decreases with increasing pH. The efficiency of degradation in aqueous medium is related to the surface charge properties of the TZC-1. The point of zero charge (pzc) for ZnO/TiO_2 is at pH 6 (Zuas, Budiman, & Hamim, 2013). The surface charge is positive at pH value lower than pH pzc, neutral at pH pzc and negative at higher pH pzc value. The surface of photocatalyst is positively charged in an acidic solution and negatively charged in alka-

line solution (Bansal *et al.*, 2015). HA consist of many phenolic and carboxylic functional groups. As is known, phenolic and carbonyl functional group can be ionized in aqueous medium and may acquire a negative charge in aqueous medium. On the other hand, the HA molecule becomes more negatively charged as pH value increases due to ionization of carboxylic and phenolic groups of humic acid (Zulfikar *et al.*, 2016). As a result, this will reduce the electrostatic attraction between the surfaces of TZC-1 and HA compounds and thus decrease the degradation efficiency of HA.

3.2.4 Effect of light distance

The influence of light distance from the surface of solution in the photocatalytic process is shown in Figure 4d. From the figure, by approaching the distance of light to the surface of the solution, the degradation percentage of HA becomes larger which indicates that the photocatalytic activity increases. It may be occurred because the light intensity is even greater if the distance of light and catalyst material becomes closer. The higher intensity facilitates the formation of hydroxyl radicals and initiates to increase the photocatalytic activity.

3.2.5 Effect of lamp power

The power of lamp also gives an effect on the photocatalytic activity which represented in Figure 4e. By increasing the power of the lamp, the degradation percentage of HA increases. Lamp power (Watt or J/s) is the amount of energy per unit of time which means the power is proportional to energy. In other words, the greater of power used will generate a large of energy (photon) that induces more electron-hole pairs on the surface catalyst which results in the higher of photocatalytic activity.

3.2.6 Comparison of photocatalytic, adsorption, and photolysis activity

According to Figure 5, by increasing the time of reaction, the percentage of degradation in photolysis curve suffered only slight changes. It can be concluded that with the conditions used in the test, HA is not degraded by the photolysis process. Different things can be seen in the adsorption curve which the percentage of HA degradation is 45.15% after 3 h of reaction indicating that ZnO can act as an adsorbent. However, when compared to the photocatalytic curve, the percentage of HA degradation gives a higher value after 3 h, i.e. 89%. These results indicate that the photocatalytic reactions show the best performance compared to photolysis and adsorption process to degrade the humic acid solution.

3.2.7 Kinetics modeling

The photocatalysis degradation kinetics of HA were studied by conducting reactions at various contents of TiO_2. Photocatalyst with as prepared samples can be expressed by degradation kinetics using the Langmuir-Hinshelwood model as follows:

$$ln\ (C_o\text{-}C_t) = k.t \quad (2)$$

where k ($hour^{-1}$) is the apparent reaction rate constant, C_o and C_t are concentration of HA (mg/L) at time t = 0 and at a given time t, respectively. The pseudo first order reaction rate constant k was calculated from the graph as shown in Figure 6 and the results are given in Table 2.

When the HA concentration is reduced to 50% of its initial value, half-life ($t_{1/2}$) of the photodegradation of the HA is calculated by substituting $C = ½.C_o$ into Equation 3:

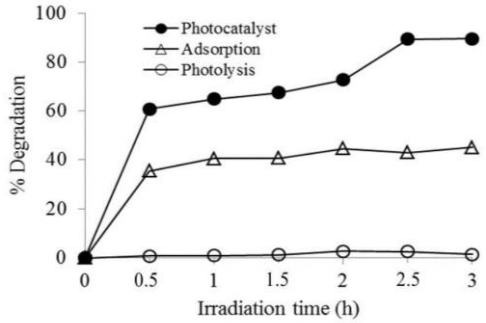

Figure 5. Comparison between photolysis, adsorption, and photocatalytic process

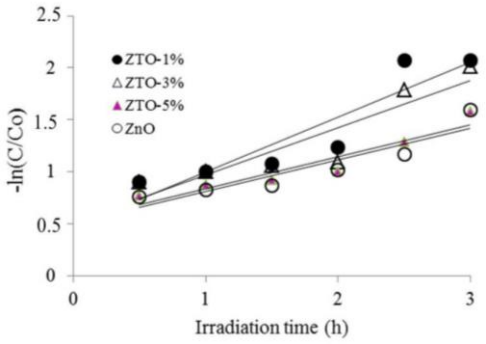

Figure 6. Pseudo-first-order kinetic plot.

Table 2. The pseudo first order reaction rate constant k and $t_{1/2}$

Sample	k ($hour^{-1}$)	$t_{1/2}$ (hour)	R^2
TZC-1	0.526	1.317	0.844
TZC-3	0.452	1.533	0.823
TZC-5	0.307	2.257	0.888
ZnO	0.306	2.265	0.851

$$\ln 2 = k.t_{1/2} \text{ or, } t_{1/2} = 0.693/k \quad (3)$$

The half-life ($t_{1/2}$) is summarized in Table 2. From the table we may conclude that the photocatalytic rate under visible radiation is directly influenced by the TiO_2 content in nanocomposite photocatalyst.

3.3 Photocatalytic activity on the real sample (peat water)

The content of peat water is dominated by humic acids which gives it a brownish color. Photocatalytic activity on the peat water was carried out by using optimum condi-

tions that has been obtained (1.40 g/L; pH 3; 15 W; the time of reaction was 3 hours; and the distance of lamp from the solution surface was 7.5 cm). Degradation of HA plot is shown in Figure 7. Photocatalytic processes can degrade the organic compounds in peat water with a percentage of degradation of 89.34%. This could imply that the concentration of organic compounds in the peat water reduces with this value. After the reaction is complete, the color of the solution changes from brownish to colorless (Figure 8) and this indicates that HA has been successfully degraded. This may indicate that photocatalytic by using nanocatalyst based TiO_2/ZnO into the peat water was successfully done.

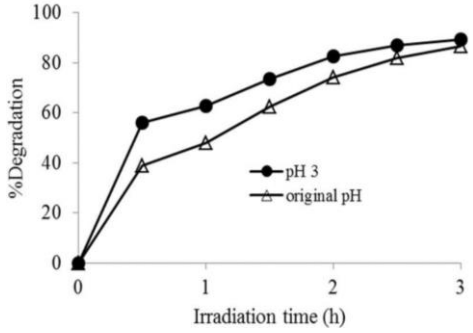

Figure 7. Photocatalytic activity on the peat water.

(a) (b)

Figure 8. Photographs of change in the color of peat water: (a) before, and (b) after treatment.

4. Conclusions

In summary, TZC photocatalysts have been successfully prepared through a sol-gel process and used for photodegradation of HA in suspension. The photocatalytic degradation rate increases with increasing catalyst dosage and light intensity. The results of the kinetic studies show that the photodegradation of HA using TZC photocatalyst could be described by the pseudo-first order kinetic model. The present study demonstrates that the TZC photocatalyst with optimal Ti content (1% of Ti) is a potential viable photocatalyst in degrading HA and possibly other pollutants (e.g. organics in water) with degradation percentage of 89.34% under visible light irradiation.

Acknowledgements

The authors are very grateful to Institut Teknologi Bandung for their financial support through Penelitian Terapan Unggulan Perguruan Tinggi 2017/2018.

References

Abbt-Braun, G., Frimmel, F. H., & Schulten, H. R. (1989). Structural investigations of aquatic humic substances by pyrolysis-field ionization mass spectrometry and pyrolysis-gas chromatography/mass spectrometry. *Water Research, 23*, 1579–1591.

Bansal, P., Chaudhary, G. R., & Mehta, S. (2015). Comparative study of catalytic activity of ZrO_2 nanoparticles for sonocatalytic and photocatalytic degradation of cationic and anionic dyes. *Chemical Engineering Journal, 280*, 475–485.

Evgenidou, E., Fytianos, K., & Poulios, I. (2005). Semiconductor-sensitized photodegradation of dichlorvos in water using TiO_2 and ZnO as catalysts. *Applied Catalysis B: Environmental, 59*, 81–89.

Huang, J., Liu, S., Kuang, L., Zhao, Y., Jiang, T., Liu, S., & Xu, X. (2013). Enhanced photocatalytic activity of quantum-dot-sensitized one-dimensionally-ordered ZnO nanorod photocatalyst. *Journal of Environmental Sciences, 25*, 2487–2491.

Janitabar-Darzi, S., & Mahjoub, A. R. (2009). Investigation of phase transformations and photocatalytic properties of sol–gel prepared nanostructured ZnO/TiO_2 composites. *Journal of Alloys and Compounds, 486*, 805 –808.

Khodadadi, B., Sabeti, M., Moradi, S., Azar, P. A., & Farshid, S. R. (2012). Synthesis of Cu-TiO_2 nanocomposite and investigation of the effectiveness of PEG, Pectin, and CMC as additives. *Journal of Applied Chemical Research, 20*, 36–44.

Lamsal, R., Montreuil, K. R., Kent, F. C., Walsh, M. E., & Gagnon, G. A. (2012). Characterization and removal of natural organic matter by an integrated membrane system. *Desalination, 303*, 12–16.

Lee, K. E., Morad, N., Teng, T. T., & Poh, B. T. (2012). Development, characterization and the application of hybrid materials in coagulation/flocculation of wastewater: A review. *Chemical Engineering Jour-nal, 203*, 370–386.

Matilainen, A., Vepsäläinen, M., & Sillanpää, M. (2010). Natural organic matter removal by coagulation during drinking water treatment: a review. *Advances in colloid and interface science, 159*, 189–197.

Metsämuuronen, S., Sillanpää, M., Bhatnagar, A., & Mänttäri, M. (2014). Natural organic matter removal from drinking water by membrane technology. *Separation and Purification Reviews, 43*, 1–61.

Moore, T. (1989) The Spectrophotometric Determination of Dissolved Organic Carbon in Peat Waters 1. *Soil Science Society of America Journal, 49*, 1590–1592.

Moradi, S., Azar, P. A., Farshid, S. R., Khorrami, S. A., & Givianrad, M. H. (2012). Effect of Additives on Characterization and Photocatalytic Activity of TiO_2/ ZnO Nanocomposite Prepared via Sol-Gel Process. *International Journal of Chemical Engineering, 20 12*, 1-5.

Nagaveni, K., Sivalingam, G., Hegde, M., & Madras, G. (20 04). Solar photocatalytic degradation of dyes: high activity of combustion synthesized nano TiO_2. *Applied Catalysis B: Environmental, 48*, 83–93.

Ng, M., Kho, E. T., Liu, S., Lim, M., & Amal, R. (2014). Highly adsorptive and regenerative magnetic TiO_2 for natural organic matter (NOM) removal in water. *Chemical Engineering Journal, 246*, 196–203.

Ng, M., Liana, A. E., Liu, S., Lim, M., Chow, C. W., Wang, D., Drikas, M., & Amal, R. (2012). Preparation and characterisation of new-polyaluminum chloride-chitosan composite coagulant. *Water Research, 46*, 46 14–4620.

Pei, C. C., & Leung, W. W. F. (2013). Photocatalytic degradation of Rhodamine B by TiO_2/ZnO nanofibers under visible-light irradiation. *Separation and purification technology, 114*, 108–116.

Perkgoz, N. K., Toru, R. S., Unal, E., Sefunc, M. A., Tek, S., Mutlugun, E., . . . Demir, H. V. (2011). Photocatalytic hybrid nanocomposites of metal oxide nanoparticles enhanced towards the visible spectral range. *Applied Catalysis B: Environmental, 105*, 77 –85.

Philippe, K. K., Hans, C., MacAdam, J., Jefferson, B., Hart, J., & Parsons, S. A. (2010). Photocatalytic oxidation of natural organic matter surrogates and the impact on trihalomethane formation potential. *Chemosphere, 81*, 1509–1516.

Pozan, G. S., & Kambur, A. (2014). Significant enhancement of photocatalytic activity over bifunctional ZnO–TiO_2 catalysts for 4-chlorophenol degradation. *Chemosphere, 105*, 152–159.

Sobana, N., & Swaminathan, M. (2007). The effect of operational parameters on the photocatalytic degradation of acid red 18 by ZnO. *Separation and Purification Technology, 56*, 101–107.

Song, L., Zhang, S., Wu, X., & Wei, Q. (2012). Controllable synthesis of hexagonal, bullet-like ZnO microstructures and nanorod arrays and their photocatalytic property. *Industrial and Engineering Chemistry Research, 51*, 4922–4926.

Štengl, V., Bakardjieva, S., & Murafa, N. (2009). Preparation and photocatalytic activity of rare earth doped TiO_2 nanoparticles. *Materials Chemistry and Physics, 114*, 217–226.

Stevenson, F., & Goh, K. (1971). Infrared spectra of humic acids and related substances. *Geochimica et Cosmochimica Acta, 35*, 471–483.

Stoyanova, A., Hitkova, H., Bachvarova-Nedelcheva, A., Iordanova, R., Ivanova, N., & Sredkova, M. (2013). Synthesis and antibacterial activity of TiO_2/ZnO nanocomposites prepared via nonhydrolytic route. *Journal of Chemical and Technology Metallurgy, 48*, 154–161.

Sukharev, V., & Kershaw, R. (1996). Concerning the role of oxygen in photocatalytic decomposition of salicylic acid in water. *Journal of Photochemistry and Photobiology A: Chemistry, 98*, 165–169.

Uddin, M. T., Nicolas, Y., Olivier, C., Toupance, T., Servant, L., Muller, M. M., . . . Jaegermann, W. (2012). Nanostructured SnO2–ZnO heterojunction photocatalysts showing enhanced photocatalytic activity for the degradation of organic dyes. *Inorganic Chemistry, 51*, 7764–7773.

Ullah, H., Khan, K. A., & Khan, W. U. (2014). ZnO/TiO_2 nanocomposite synthesized by sol gel from highly soluble single source molecular precursor. *Chinese Journal of Chemical Physics, 27*, 548–554.

Wang, C., Xu, B. Q., Wang, X., & Zhao, J. (2005). Preparation and photocatalytic activity of ZnO/TiO_2/SnO2 mixture. *Journal of Solid State Chemistry, 178*, 35 00–3506.

Wang, X., Zhang, Q., Wan, Q., Dai, G., Zhou, C., & Zou, B. (2011). Controllable ZnO architectures by ethanolmine-assisted hydrothermal reaction for enhanced photocatalytic activity. *The Journal of Physical Chemistry C, 115*, 2769–2775.

Zouboulis, A. I., Chai, X. L., & Katsoyiannis, I. A. (2004). The application of bioflocculant for the removal of humic acids from stabilized landfill leachates. *Journal of Environmental Management, 70*, 35–41.

Zuas, O., Budiman, H., & Hamim, N. (2013). Synthesis of ZnO nanoparticles formicrowave induced rapid catalytic decolorization of congo red dye. *Advanced Materials Letters, 4*, 662–667.

Zulfikar, M. A., Afrita, S., Wahyuningrum, D., & Ledyastuti, M. (2016). Preparation of fe3o4-chitosan hybrid nano-particles used for humic acid adsorption. *Environmental Nanotechnology, Monitoring and Management, 306*(6), 64–75.

Zulfikar, M., Suri, F., Rusnadi., Setiyanto, H., Mufti, N., Ledyastuti, M., & Wahyuningrum, D. (2016). Fe_3O_4 nano-particles prepared by co-precipitation method using local sands as a raw material and their application for humic acid removal. *International Journal of Environmental Studies, 73*, 79–94.

Zulfikar, M., Afrianingsih, I., Nasir, M., & Handayani, N. (20 17). Fabrication of a nanofiber membrane functionalized with molecularly imprinted polymers for humic acid removal from peat water. *Desalination and Water Treatment, 97*, 203–212.

Zulfikar, M., Wahyuningrum, D., Mukti, R., & Setiyanto, H. (2016). Molecularly imprinted polymers (MIPs): a functional material for removal of humic acid from peat water. *Desalination and Water Treatment, 57*, 15164–15175